

RSC Advances



This is an *Accepted Manuscript*, which has been through the Royal Society of Chemistry peer review process and has been accepted for publication.

Accepted Manuscripts are published online shortly after acceptance, before technical editing, formatting and proof reading. Using this free service, authors can make their results available to the community, in citable form, before we publish the edited article. This *Accepted Manuscript* will be replaced by the edited, formatted and paginated article as soon as this is available.

You can find more information about *Accepted Manuscripts* in the [Information for Authors](#).

Please note that technical editing may introduce minor changes to the text and/or graphics, which may alter content. The journal's standard [Terms & Conditions](#) and the [Ethical guidelines](#) still apply. In no event shall the Royal Society of Chemistry be held responsible for any errors or omissions in this *Accepted Manuscript* or any consequences arising from the use of any information it contains.

Novel soluble thieno[3,2-b]thiophene fused porphyrazine

 Abby Casey^a, Yang Han^a, Mark F. Wyatt^b, Thomas D. Anthopoulos^c and Martin Heeney^a

 Received 00th January 20xx,
 Accepted 00th January 20xx

DOI: 10.1039/x0xx00000x

www.rsc.org/

The synthesis of the first soluble thieno[3,2-b]thiophene based porphyrazine (ZnTTPz) is reported from the cyclisation of 2,3-dicyano-5-octylthieno[3,2-b]thiophene. ZnTTPz can be considered the all thiophene analogue of naphthalocyanine. ZnTTPz exhibits a red-shifted absorption in solution and thin film, as well as a reduced band gap in comparison to the thiophene analogue due to an increased conjugation length. Films of ZnTTPz processed from solution exhibit p-type semiconducting behaviour in field-effect transistors with low hysteresis and reasonable charge carrier mobility.

Introduction

The intensely coloured macrocycle phthalocyanine (Pc) has traditionally been used as a dye material but more recently has attracted attention as the active semiconducting component in a range of organic electronic devices. The high absorption coefficient, small optical band gap and strong π - π stacking in the solid state are all attractive properties for high performance organic semiconductor (OSC) materials.^{1–5} Phthalocyanines and their derivatives also typically exhibit high photo, air, thermal and chemical stability which are desirable properties for electronic devices.

Phthalocyanine consists of four benzenoid units fused to a central porphyrazine (Pz) core. Changing the type of aromatic group fused to the Pz core greatly influences the optoelectronic properties and solid state packing of the material. For instance, replacing the benzene groups (phthalocyanine - Pc) for naphthalene (naphthalocyanine - Nc) results in a significant red shift of the Q-band absorption (HOMO-LUMO transition) into the near-IR region. There are two regioisomers of naphthalocyanine: 2,3-Nc made from 2,3-dicyanonaphthalene in which the rings are linearly annulated, and 1,2-Nc made from 1,2-dicyanonaphthalene in which the rings are angularly annulated. The magnitude of the Q-band shift is strongly dependent on the nature on this annulation. In addition, whilst 2,3-Ncs exist as a single isomer, 1,2-Ncs have four possible isomeric structures of C_{4h} , C_s , C_{2v} and D_{2h} symmetry.^{6,7} The replacement of the benzenoid units with heterocyclic groups is another route to tune the properties of the ring.^{8–12} For instance the incorporation of electron rich heterocycles such as thiophene (TPz)¹³ or selenophene (SePz)¹⁴ results in materials showing promising p-type

charge carrier mobility in transistor devices.

Inspired by the promising transistor performance of TPz we have looked at extending the conjugation length by replacing thiophene with fused thieno[3,2-b]thiophene to form TTPz. TPz and TTPz can be considered the thiophene analogues of Pc and NPc respectively. More accurately TTPz can be considered as the thiophene analogue of 1,2-Nc as it also exists as four isomers with C_{4h} , C_s , C_{2v} and D_{2h} symmetry. Replacing the sulfur heteroatom in TTPz with vinyl groups directly leads to 1,2-Nc (see Figure 1).

Herein, we report the first synthesis of ZnTTPz, and compare its optoelectronic properties to the reported properties of ZnPc¹⁵, Zn-1,2-Nc¹⁶, Zn-2,3-Nc¹⁷ and an alkylated derivative of ZnTPz¹⁸. We also report the preliminary transistor performance in bottom gate transistor devices.

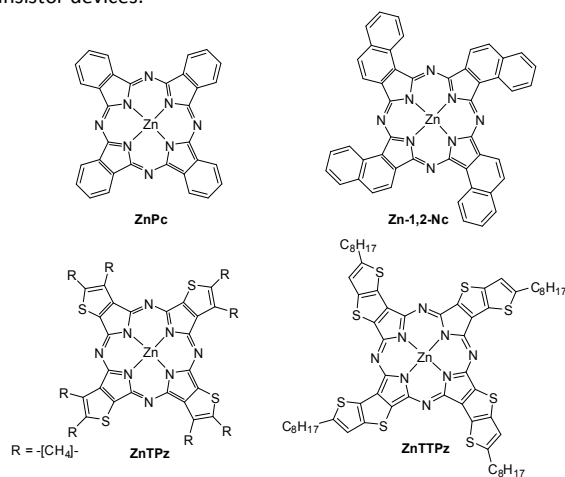


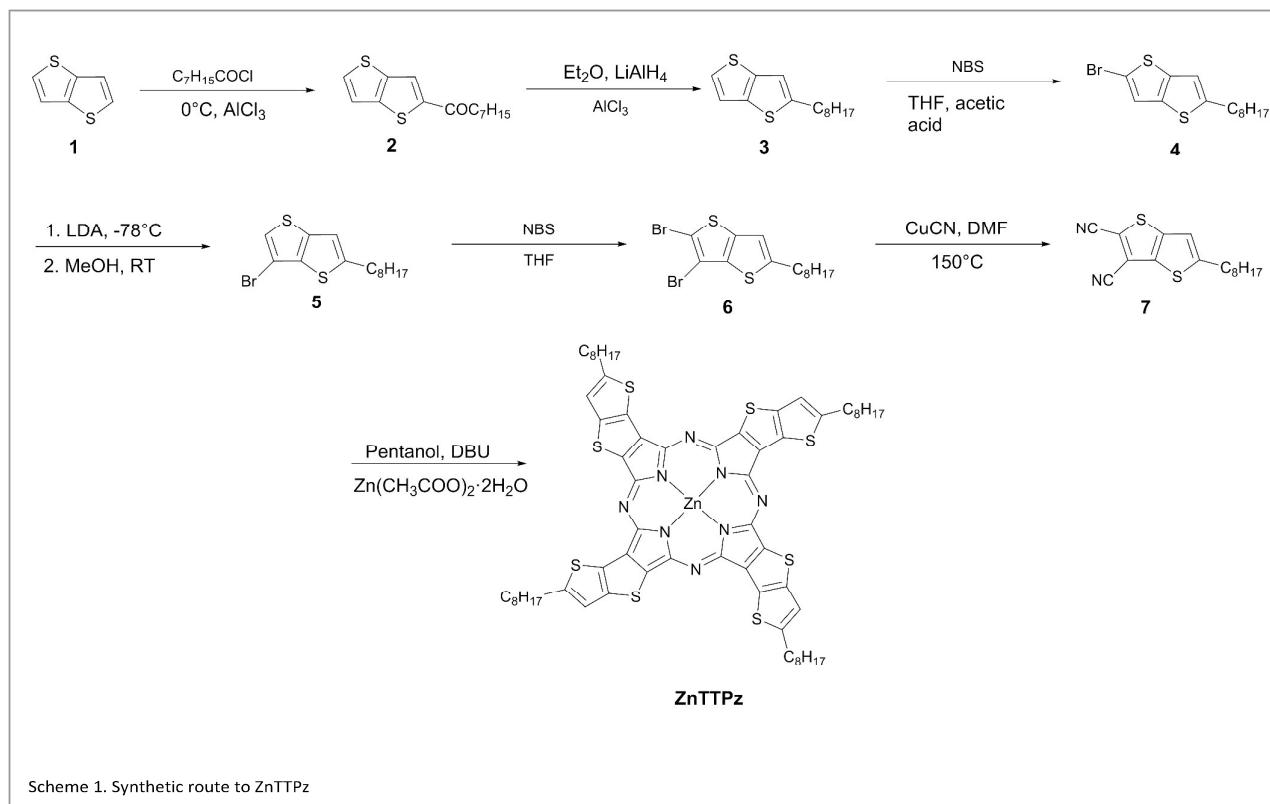
Figure 1: Structures of zinc phthalocyanine (ZnPc), zinc-1,2-naphthalocyanine (Zn-1,2-Nc), tetrahydrobenzothiophene-fused porphyrazine (ZnTPz)¹⁸ and zinc 5-octylthienothiophene-fused porphyrazine (ZnTTPz).

^a Dept. Chemistry and Centre for Plastic Electronics, Imperial College London, London SW7 2AZ, U.K.

^b EPSRC UK National Mass Spectrometry Facility (NMSF), Swansea University Medical School, Singleton Park, Swansea, SA2 8PP U.K.

^c Department of Physics and Centre for Plastic Electronics Imperial College London SW7 2AZ, U.K.

Electronic Supplementary Information (ESI) available: CV's, DSC, NMRs and mass spectra. See DOI: 10.1039/x0xx00000x



Results and Discussion

The synthesis of ZnTTPz is shown in Scheme 1. Octyl groups were added to the ring periphery to ensure solution processability in the final macrocycle. Thus octanoyl groups were introduced to the 2 position of thieno[3,2-*b*]thiophene via a Friedel-Crafts acylation to form **2**, which was subsequently reduced using LiAlH₄ and AlCl₃ to produce the saturated octyl chain on molecule **3**. Bromination of **3** using NBS in THF and acetic acid afforded 2-bromo-5-octylthieno[3,2-*b*]thiophene in good yield. Since subsequent bromination occurred adjacent to the octyl chain, a base-catalysed halogen-dance reaction was utilised to rearrange the bromine from the 2-position to the 3-position forming **5**. Subsequent bromination of the most reactive 2-position formed the dibrominated product **6**. The dicyano precursor **7** was then formed via the Rosenmund von Braun cyanation by reaction with copper cyanide in refluxing DMF. Formation of the hydro-debrominated side product and a small amount of copper 5-octylthieno[3,2-*b*]thiophene-fused porphyrazine reduced the yield of step 6 to ~50%. The final step involved a template directed cyclisation around zinc, initiated by DBU to form the final product zinc 5-octylthieno[3,2-*b*]thiophene-fused porphyrazine (ZnTTPz).

Fusing the thieno[3,2-*b*]thiophene unit to the porphyrazine core via the 2,3 positions gives rise to four possible structural isomers, (see Figure 2). The final cyclisation step forming the porphyrazine ring is expected to give a mixture of all four isomers due to a lack of selectivity. When synthesising CuTPz Takimiya and co-workers also made a mixture of isomers that could not be separated. Unlike CuTPz each isomer of ZnTTPz is structurally very different, resulting in the alkyl chains of each isomer pointing in different directions to

the alkyl chains of the other isomers (see Figure 2). However, despite the structural dissimilarity of the isomers we were still unable to separate them by column chromatography or size-exclusion chromatography. ¹H NMR spectroscopy of ZnTTPz gave broad signals presumably due to the presence of the different isomers, the aromatic protons on the thienothiophene unit gave broad signals between 6.44 and 5.94 ppm (see Figure S7).

Table 1 compares both the experimental and theoretically calculated excitation energies of ZnTPz, ZnTTPz, ZnPc, Zn-1,2-Nc and Zn-2,3-Nc. DFT calculations, performed with a B3LYP level of theory and basis set of 631G(d), were used to approximate the excitation energies. DFT calculations for both ZnTPz and ZnTTPz were carried out on the C_{4h} isomer. The UV/Vis spectra of ZnTTPz in both chloroform solution and as a thin film are shown in Figure 3a. As is typical with porphyrazine derivatives ZnTTPz shows two main absorptions, the B-band in the blue region at 370 nm and the Q-band in the red region at 693 nm which corresponds to the HOMO-LUMO transition. The Q-band of ZnTTPz peaked at 689 nm in THF, a significant red-shift of 24 nm in comparison to a derivative of ZnTPz with cyclic tetrahydrobenzo solubilising groups, which had an absorption maximum at 665 nm in THF according to literature¹⁸. For further comparison, the Q band of alkylated CuTPz absorbs at 657 nm in toluene.¹³ The red-shift can be attributed to the extension of the conjugation length caused by substituting the thiophene in ZnTPz for thieno[3,2-*b*]thiophene in ZnTTPz.

Upon film formation the Q-band of ZnTTPz broadens to both the blue and red regions either side of the solution Q-band. This suggests the formation of both cofacial H-aggregates and J-aggregates in the film, accounting for the blue and red shifts respectively. The absorption maximum of ZnTTPz in thin film was 710 nm, a red shift of 17 nm from chloroform solution. The optical

band gap, measured from the absorption onset in thin film, had a value of 1.42 eV. ZnTTPz had a high molar extinction coefficient (ϵ) of 131,000 $\text{M}^{-1}\text{cm}^{-1}$ (693 nm) in chloroform solution. The absorbance and photoluminescence spectra of ZnTTPz in chloroform solution are compared in Figure 3b. The narrow absorption band of ZnTTPz is mirrored with a narrow emission band red shifted by 11 nm. Small Stokes shifts are characteristic of phthalocyanine and its derivatives; the rigidity of these molecules means there is little structural rearrangement between the ground state and excited state geometries.

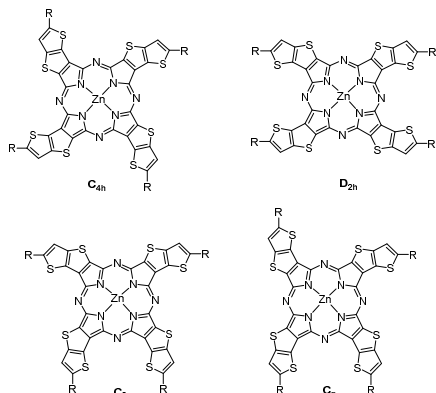


Figure 2: The four possible structural isomers of ZnTTPz

It is interesting to note that whilst the experimental λ_{max} of ZnTPz¹⁸ is slightly blue shifted in comparison to ZnPc¹⁵ (both in THF according to literature), the peak absorption of ZnTTPz is *red-shifted* by 12 nm in comparison to the λ_{max} of Zn-1,2-Nc reported in the literature (both in DMSO see Table 1). These observations are supported by DFT calculations (see Table 1). Although DFT calculations approximated the excitation energies of the molecules to be much higher than those measured experimentally, accurate trends in band gaps shifts between molecules were predicted. For instance DFT calculations predict the ZnTPz λ_{max} to be *blue* shifted by 12 nm in comparison to ZnPc and the ZnTTPz λ_{max} to be *red* shifted by 17 nm in comparison to Zn-1,2-Nc which compares fairly well with the experimentally observed data. Linear annulation of the benzene rings in Nc (2,3-Nc) is known to lead to strongly red-shifted Q-bands in comparison to angularly annulated Nc (1,2-Nc).¹⁹ We also observe that the Q-band of ZnTTPz is significantly blue shifted (70 nm) in comparison to the λ_{max} of Zn-2,3-Nc reported in the literature.¹⁷ DFT calculations once again accurately predict this large red shift, estimating it to be 63 nm (see Table 1).

Molecule	Experimental λ_{max} (nm)	Excitation energy (nm) B3LYP/ 631G(d)
ZnTPz ^{a,18}	665 ^b	581
ZnTTPz	689 ^b , 696 ^c	631
ZnPc ¹⁵	668 ^b , 672 ^c	593
Zn-1,2-Nc ¹⁶	684 ^c	614
Zn-2,3-Nc ¹⁷	766 ^c	694

Table 1: Optical properties of phthalocyanine derivatives ^aexperimental λ_{max} is for tetrahydrobenzo substituted ZnTPz¹⁸ ^b λ_{max} of absorption spectra in THF ^c λ_{max} of absorption spectra in DMSO.

The electrochemical properties of ZnTTPz were investigated using cyclic voltammetry. The cyclic voltammograms for ZnTTPz are shown in Figure S1. The oxidation peak of ZnTTPz appeared to be

partially reversible and the HOMO level was therefore estimated from the half wave oxidation potential ($E_{1/2}$) giving a value of -5.02 eV. The reduction peak however was irreversible and the LUMO level was therefore estimated from the onset of first reduction, giving a value of -3.44 eV. The electrical band gap of ZnTTPz was therefore 1.58 eV, having a slightly larger value than the optical band gap of 1.42 eV which does not take into account exciton binding energy. The ionisation potential of ZnTTPz in thin film was measured using photoelectron spectroscopy in air (PESA) and had a value of -5.08 eV. Due to the longer conjugation length of ZnTTPz, the ionisation potential is raised in energy by ~ 0.1 eV in comparison to copper 5-hexylthiophene-fused porphyrazine (CuTPz), which according to PESA measurements in the literature had an ionisation potential of -5.20 eV.¹³ The central metal atom in phthalocyanines has little reported effect on the energy of the HOMO level.²⁰

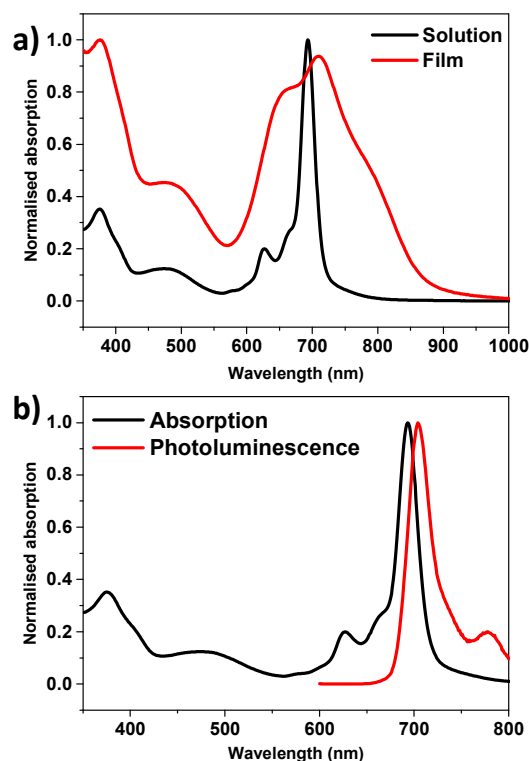


Figure 3: a) absorbance spectroscopy of ZnTTPz in chloroform solution and in thin film b) absorbance and photoluminescence spectroscopy of ZnTTPz in chloroform solution.

The transistor performance of ZnTTPz was investigated in bottom gate, top contact OFET devices. Gold source drain electrodes were used and the Si/SiO₂ dielectric was treated with OTS prior to semiconductor deposition. As-spun films of ZnTTPz from chloroform showed P-type charge transport with hole mobilities on the order of 10^{-5} cm^2/Vs with a peak performance of 4.3×10^{-5} cm^2/Vs . Annealing films at 100 °C improved the hole mobility by 2 orders of magnitude to $\sim 10^{-3}$ cm^2/Vs with a peak performance of 7.8×10^{-3} cm^2/Vs . The transfer characteristics for these devices are shown in Figure 4. The mobility of ZnTTPz is reduced in comparison to other porphyrazines fused with electron rich five membered rings such as

thiophene which gave hole mobilities of 0.1-0.2 cm²/Vs and selenophene which had mobilities on the order of 10⁻² cm²/Vs. This is likely to be due to disorder imparted by the mixture of structurally dissimilar isomers (see Figure 2). In the case of thiophene and selenophene fused porphyrazines the alkyl chain in the 5-position remains in a similar position with respect to the other isomers allowing crystalline, ordered films. ZnTTPz however appears to be amorphous with no obvious transitions in differential scanning calorimetry traces (see Figure S2) and no crystalline behaviour observed using polarised optical microscopy at different temperatures. Whilst this may hinder OFET devices, it may benefit solar cell applications to have a less crystalline donor to encourage mixing with PC₆₁BM. For example solar cells made using CuTPz gave poor performance (PCE = 0.13%) due to large domains of the crystalline donor limiting the large donor acceptor interface required for high performance BHJ devices.²¹ We note that although ZnTTPz is a mixture of isomers, some previous studies have shown that phthalocyanine or porphyrin mixtures can outperform single isomers.^{22,23} The reduced band gap of ZnTTPz in comparison to CuTPz is also likely to improve solar cell performance through increased photocurrent.

solar cell performance through increased photocurrent. ZnTTPz is a p-type semiconductor exhibiting reasonable mobility in field-effect transistor devices. TPz and TTPz also provide an interesting optical comparison with Pc and 1,2-Nc and help to further our understanding of the role of thiophene and benzene aromaticity in conjugated materials.

Experimental Section

General: All solvents and chemicals, were purchased from Sigma-Aldrich and used without further purification. 1-(Thieno[3,2-*b*]thiophen-2-yl)octan-1-one and 2-octylthieno[3,2-*b*]thiophene were made according to literature.²⁴ All reactions were performed under an Argon atmosphere. Nuclear magnetic resonance (NMR) spectra were recorded on Bruker AV-400 (400 MHz) spectrometers in chloroform-*d* solutions. UV-Visible absorption spectra were measured using a Shimadzu UV-1800 UV-Vis Spectrophotometer. Solutions in chloroform (5 mg/mL) were used to spin coat thin films at 1000 rpm for 60 seconds. Solutions were not de-oxygenated for these measurements. Ionisation potentials were measured by Photo-electron Spectroscopy in Air (PESA) on a Riken Keiki AC-2 PESA spectrometer. ZnTTPz thin films were prepared by spin-coating from chloroform (5 mg/mL) onto glass substrates. The PESA samples were run with a light intensity of 5 nW and data processed with a power number of 0.5. Density functional theory using a B3LYP functional and basis set of 6-31G(d)²⁵ as used to calculate the different molecules HOMO levels, whilst TD-DFT was used to calculate excitation energies. All calculations were carried out using Gaussview 5.0. Cyclic voltammograms were recorded using a Metrohm Autolab PGStat101 Potentiostat/Galvanostat. The experimental set-up consisted of an Ag/Ag⁺ reference electrode, a platinum mesh counter electrode and a platinum wire working electrode. Experiments were carried out in solutions of 0.3 M tetrabutylammonium hexafluorophosphate ([n-Bu₄N]PF₆) electrolyte in DCM containing 10⁻⁴M of ZnTTPz at room temperature under argon. A scanning rate of 0.1 Vs⁻¹ was used. A ferrocene internal standard was used to calibrate the results assuming that the ferrocene/ferrocenium reference redox system is 4.8 eV below the vacuum level.

MALDI-TOF MS spectra were acquired using an UltrafleXtreme MALDI-TOF mass spectrometer (Bruker Daltonics, Bremen, Germany), which is equipped with a Nd:YAG laser ($\lambda = 355$ nm). Data were acquired using flexControl software v3.4, while post-acquisition processing of data was performed by flexAnalysis software v3.4. MALDI matrix trans-2-[3-(4-tert-butylphenyl)-2-methyl-2-propenylidene]malononitrile (DCTB) was purchased from Insight Biotechnology Ltd. (Wembley, U.K.). Poly (propylene glycol) standard (average molecular weight ~ 1000 , PPG1000), tetrahydrofuran (THF; BHT stabilised) and sodium acetate (NaOAc) additive were purchased from Sigma-Aldrich (Poole, U.K.). Dichloromethane (DCM) and methanol (MeOH) solvents were purchased from Fisher Scientific (Loughborough, U.K.). DCTB matrix was dissolved in DCM at 20 mg/mL, while the sample ZnTTPz was prepared in DCM at 1 mg/mL. PPG1000 was prepared in THF at 10 mg/mL and NaOAc was solvated in MeOH at 10 mg/mL; the PPG solution was mixed in a 20:1 ratio with NaOAc to form calibration standard solutions. For initial externally calibrated MALDI characterisation analysis, the ZnTTPz sample was prepared by mixing with DCTB in a 1:49 ratio; 0.5 μ L of this mixture solution was spotted onto the MALDI plate and dried in air. MALDI data was

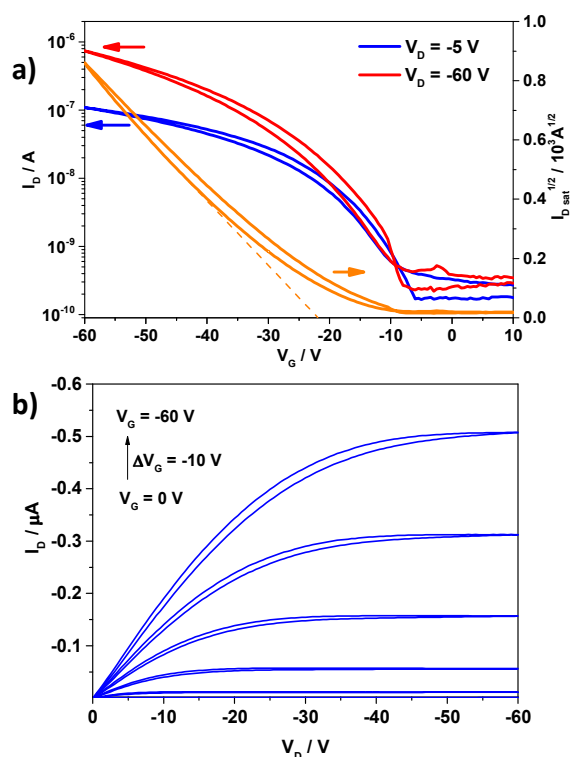


Figure 4: a) Transfer and b) output characteristics of ZnTTPz under negative voltages in the BG/TC device configuration after annealing at 100 °C. The channel width and length of the transistors are 1000 μ m and 30 μ m, respectively.

Conclusions

In conclusion we have synthesised the first thienothiophene based porphyrazine (ZnTTPz) which shows a significant red-shift in absorption in comparison to the thiophene analogue ZnTPz. The reduced bandgap of ZnTTPz in comparison to ZnTPz may improve

acquired in positive-reflectron mode. MALDI accurate mass measurement was performed via mixing (ZnTTPz)-DCTB solution with PPG1000 calibration solution, such that the ion intensity of both sample and standard were approximately equivalent when analysed. Acquired data was internally calibrated using the cubic enhanced function from six PPG species bracketing the sample species.

OFET device fabrication

Bottom gate/top contact devices were fabricated on heavily doped n^+ -Si (100) wafers with 400 nm-thick thermally grown SiO₂. The Si/SiO₂ substrates were treated with OTS to form a self-assembled monolayer. All polymers were dissolved in chloroform (0.2 wt%) and spin cast at 2000 rpm for 60 s. The film was either annealed at 100°C for 30 min or processed without annealing. Au (30 nm) source and drain electrodes were deposited under vacuum through shadow masks. The channel width and length of the transistors are 1000 μ m and 30 μ m, respectively. Mobility was extracted from the slope of $I_D^{1/2}$ vs. V_G .

Synthesis:

2-Bromo-5-octylthieno[3,2-*b*]thiophene (4)

A mixture of 3 (3.31 g, 13.12 mmol) and NBS (2.48 g, 13.90 mmol) in acetic acid (10 mL) and THF (40 mL) was stirred in the dark for 24 hours. The mixture was poured into an aqueous solution of sodium sulphite (100 mL) and extracted with DCM (2 x 30 mL). The combined organics were dried (MgSO₄), filtered and concentrated under reduced pressure. The crude product was purified by column chromatography over silica (eluent: hexane) to afford 4 as a yellow oil (89%, 3.92 g). ¹H NMR (400 MHz, CDCl₃) δ 7.17 (d, J = 0.5 Hz, 1H), 6.86 – 6.85 (m, 1H), 2.87 – 2.81 (m, 2H), 1.73 – 1.65 (m, 2H), 1.41 – 1.23 (m, 10H), 0.88 (t, J = 7.1 Hz, 3H). ¹³C NMR (101 MHz, CDCl₃) δ 148.06, 138.98, 136.09, 122.29, 116.03, 111.44, 32.00, 31.67, 31.07, 29.45, 29.35, 29.20, 22.81, 14.25. MS (EI) m/z = 332 (M⁺).

3-Bromo-5-octylthieno[3,2-*b*]thiophene (5)

To a solution of diisopropyl amine (1.735 g, 17.14 mmol) in anhydrous THF (25 mL) at -78°C was added *n*-BuLi (6.86 mL of 2.5M solution in hexanes, 17.14 mmol). The reaction mixture was stirred at -78°C for 20 min, warmed to room temperature and then cooled again to -78°C. The solution of LDA was then added dropwise to a solution of 3 (2.8 g, 8.49 mmol) in THF (5 mL) at -78°C. The reaction was stirred at -78°C for 2 h then quenched with methanol and stirred for another hour whilst warming to room temperature. Brine (50 mL) was then added to the mixture and the product extracted using Et₂O (2 x 30 mL). The combined organics were washed with water, dried (MgSO₄), filtered and the solvent removed under reduced pressure. The crude product was purified by column chromatography over silica (eluent: hexane) to afford 5 as a yellow oil (76%, 2.13 g). ¹H NMR (400 MHz, CDCl₃) δ 7.16 – 7.15 (s, 1H), 6.98 – 6.97 (t, J = 0.9 Hz, 1H), 2.91 – 2.85 (m, 2H), 1.76 – 1.66 (m, 2H), 1.43 – 1.22 (m, 10H), 0.88 (t, J = 7.1 Hz, 3H). ¹³C NMR (101 MHz, CDCl₃) δ 149.96, 138.52, 138.08, 122.16, 117.28, 102.57, 32.00, 31.69, 31.43, 29.46, 29.35, 29.18, 22.81, 14.26. MS (EI) m/z = 332 (M⁺).

2,3-Dibromo-5-octylthieno[3,2-*b*]thiophene (6)

A mixture of 4 (2.132 g, 6.43 mmol) and NBS (1.20 g, 6.75 mmol) in THF (40 mL) was stirred in the absence of light for 24 h. The mixture was poured into an aqueous solution of sodium sulphite (100 mL)

and extracted with DCM (2 x 30 mL). The combined organics were dried (MgSO₄), filtered and the solvent removed under reduced pressure. The crude product was purified by column chromatography over silica (eluent: hexane) to afford 6 as a clear oil (70 %, 1.8 g). ¹H NMR (400 MHz, CDCl₃) δ 6.91 (t, J = 1.0 Hz, 1H), 2.88 – 2.83 (m, 2H), 1.74 – 1.66 (m, 2H), 1.41 – 1.21 (m, 10H), 0.88 (t, J = 7.1 Hz, 3H). ¹³C NMR (101 MHz, CDCl₃) δ 148.88, 137.34, 136.54, 116.99, 109.97, 106.54, 31.99, 31.63, 31.16, 29.43, 29.33, 29.15, 22.81, 14.25. MS (EI) m/z = 410 (M⁺).

2,3-Dicyano-5-octylthieno[3,2-*b*]thiophene (7)

CuCN (2.55 g, 28.5 mmol) and 5 (1.46 g, 3.56 mmol) were added to a 25 mL round bottomed flask. The flask was then fitted with a reflux condenser and degassed with argon. Degassed DMF (8 mL) was added and the mixture refluxed for 4 h. The reaction was then cooled to 80°C and FeCl₃·6H₂O (7.7 g, 28.5 mmol) added. The mixture was stirred for 30 min before allowing to cool to room temperature. Water was added to the mixture and the residue filtered and washed thoroughly with water. The aqueous phase was extracted with DCM (2 x 50 mL) before being quenched with concentrated ammonia hydroxide solution. 6M HCl (50 mL) was then added to the solid residue and the mixture left stirring at 60°C for 2 hours (careful! Any residual CuCN left will form HCN gas upon contact with HCl). The product was then extracted from the acidic mixture with DCM. The organic layers were then combined, the solvent removed under reduced pressure and the crude product purified by column chromatography over silica (eluent: EtOAc/Hexane 1:9, v:v) to afford 7 as a pale green oil which solidified upon standing (522 mg, 48%). ¹H NMR (400 MHz, CDCl₃) δ 7.05 (s, 1H), 2.96 (t, J = 7.5 Hz, 2H), 1.79 – 1.69 (m, 2H), 1.44 – 1.20 (m, 10H), 0.86 (t, J = 7.1 Hz, 3H). ¹³C NMR (101 MHz, CDCl₃) δ 158.08, 142.88, 137.13, 116.64, 115.98, 111.98, 111.81, 111.34, 31.86, 31.64, 31.25, 29.27, 29.20, 29.05, 22.70, 14.16. MS (EI) m/z = 302.09 (M⁺).

Zinc 5-Octylthieno[3,2-*b*]thiophene-fused porphyrazine (ZnTTPz)

To a refluxing solution of 6 (0.250 g, 0.828 mmol) in dry pentanol (5mL) was added DBU (88 mg, 0.579 mmol). After one hour, zinc acetate dihydrate (99.999% zinc, 55 mg, 0.248 mmol) was added and the mixture refluxed for a further 18 h. The mixture was cooled to room temperature before methanol (20 mL) was added. The resulting precipitate was filtered and washed with more methanol (2 x 20 mL). The crude precipitate was then purified by column chromatography over silica (eluent: THF/hexane 1:9, v:v) to afford ZnTTPz as a dark green solid (20 mgs, 7.6%). ¹H NMR (400 MHz, CDCl₃) δ 6.44 – 5.94 (br, 4H), 2.66-2.33 (br, 4H), 2.28-2.20 (br, 4H), 1.68-1.40 (br, 8H), 1.39 – 1.15 (br, 40H), 0.98 – 0.85 (br, 12H). UV-Vis λ_{max} (CHCl₃): 693 (131,000 M⁻¹cm⁻¹) nm. Accurate mass measurement (C₆₄H₇₂N₈S₈Zn, MALDI-TOF): calculated for M⁺ isotopic cluster at m/z = 1272.2932, found 1272.2914 (see Figure S9).

Acknowledgements

We thank the UK's Engineering and Physical Sciences Research Council (EPSRC) for financial support via the Doctoral Training Centre in Plastic Electronics EP/G037515/1. We gratefully acknowledge Dr Scott E. Watkins (CSIRO) for the PESA measurements.

Notes and references

1. O. Melville, B. H. Lessard, and T. P. Bender, *ACS Appl. Mater. Interfaces*, 2015, **7**, 13105–13118.
2. Y. Lin, Y. Li, and X. Zhan, *Chem. Soc. Rev.*, 2012, **41**, 4245–72.
3. C. G. Claessens, U. Hahn, and T. Torres, *Chem. Rec.*, 2008, **8**, 75–97.
4. M. V. Martínez-Díaz, G. de la Torre, and T. Torres, *Chem. Commun.*, 2010, **46**, 7090–108.
5. G. de la Torre, C. G. Claessens, and T. Torres, *Chem. Commun.*, 2007, 2000–2015.
6. V. M. Negrimovskii, M. Bouvet, E. a. Luk'Yanets, and J. Simon, *J. Porphyrins Phthalocyanines*, 2001, **05**, 423–427.
7. V. M. Negrimovskii, M. Bouvet, E. a. Luk'Yanets, and J. Simon, *J. Porphyrins Phthalocyanines*, 2000, **04**, 248–255.
8. E. M. Bauer, D. Cardarilli, C. Ercolani, P. a. Stuzhin, and U. Russo, *Inorg. Chem.*, 1999, **38**, 6114–6120.
9. E. M. Bauer, C. Ercolani, P. Galli, I. A. Popkova, and P. A. Stuzhin, *J. Porphyrins Phthalocyanines*, 1999, **3**, 371–379.
10. P. A. Stuzhin, E. M. Bauer, and C. Ercolani, *Inorg. Chem.*, 1998, **37**, 1533–1539.
11. P. A. Stuzhin, M. S. Mikhailov, E. S. Yurina, M. I. Bazanov, O. I. Koifman, G. L. Pakhomov, V. V. Travkin, and A. a. Sinelshchikova, *Chem. Commun.*, 2012, **48**, 10135–10137.
12. M. P. Donzello, C. Ercolani, K. M. Kadish, G. Ricciardi, A. Rosa, and P. A. Stuzhin, *Inorg. Chem.*, 2007, **46**, 4145–4157.
13. E. Miyazaki, A. Kaku, H. Mori, M. Iwatani, and K. Takimiya, *J. Mater. Chem.*, 2009, **19**, 5913–5915.
14. M. Shahid, N. Padamsey, J. Labram, T. D. Anthopoulos, and M. Heeney, *J. Mater. Chem. C*, 2013, **1**, 6198–6201.
15. A. Ogunsipe, D. Maree, and T. Nyokong, *J. Mol. Struct.*, 2003, **650**, 131–140.
16. R. T. Kuznetsova, N. S. Savenkova, G. V. Maier, S. M. Arabei, T. A. Pavich, and K. N. Solov'ev, *J. Appl. Spectrosc.*, 2007, **74**, 485–493.
17. A. Ogunsipe, J. Chen, and T. Nyokong, *New J. Chem.*, 2004, **28**, 822–827.
18. T. V. Dubinina, D. V. Dyumaeva, S. a. Trashin, M. V. Sedova, A. S. Dudnik, N. E. Borisova, L. G. Tomilova, and N. S. Zefirov, *Dye. Pigment.*, 2013, **96**, 699–704.
19. V. V. Sapunov, K. N. Solov'ev, and M. G. Gal'pern, *Theor. Exp. Chem.*, 1991, **26**, 551–555.
20. M.-S. Liao and S. Scheiner, *J. Chem. Phys.*, 2001, **114**, 9780–9791.
21. H. Mori, E. Miyazaki, I. Osaka, and K. Takimiya, *Org. Electron.*, 2012, **13**, 1975–1980.
22. A. Varotto, C.-Y. Nam, I. Radivojevic, J. P. C. Tomé, J. a S. Cavaleiro, C. T. Black, and C. M. Drain, *J. Am. Chem. Soc.*, 2010, **132**, 2552–4.
23. Y. Zhen, H. Tanaka, K. Harano, S. Okada, Y. Matsuo, and E. Nakamura, *J. Am. Chem. Soc.*, 2015, **137**, 2247–2252.
24. F. Gao, Y. Wang, J. Zhang, D. Shi, M. Wang, R. Humphry-Baker, P. Wang, S. M. Zakeeruddin, and M. Grätzel, *Chem. Commun.*, 2008, 2635–7.
25. A. D. Becke, *J. Chem. Phys.*, 1993, **98**, 5648–5652.